

# BR( $\bar{B} \rightarrow X_s \gamma$ ): First Next-to-Next-to-Leading Order Results

Matthias Steinhauser<sup>a \*</sup>

<sup>a</sup>II. Institut für Theoretische Physik, Universität Hamburg,  
Luruper Chaussee 149, D-22761, Hamburg, Germany.

In this contribution the first next-to-next-to-leading order corrections to the branching ratio BR( $\bar{B} \rightarrow X_s \gamma$ ) are discussed. This includes the completion of the matching part and the fermionic corrections to the most important operator matrix elements.

## 1. Motivation

The rare decay of a  $\bar{B}$  meson into a meson containing a strange quark and a photon is very sensitive to new physics which is connected to the fact that in the Standard Model (SM) this process is loop-induced. Thus a precise comparison of theoretical calculations and experimental measurements can lead to important hints on the theory beyond the SM. Conventionally the decay is normalized to the semileptonic  $B$ -meson decay. The corresponding branching ratio has meanwhile been measured by CLEO [1], ALEPH [2], BELLE [3] and BABAR [4] which is summarized in Fig. 1 and leads to the experimental world average<sup>2</sup> [5]

$$\text{BR}[\bar{B} \rightarrow X_s \gamma, (E_\gamma > m_b/20)] = (3.42 \pm 0.30) \times 10^{-4}. \quad (1)$$

This result agrees very well with the SM predictions [6, 7]

$$\begin{aligned} \text{BR}[\bar{B} \rightarrow X_s \gamma, (E_\gamma > 1.6 \text{ GeV})] &= (3.57 \pm 0.30) \times 10^{-4}, \\ \text{BR}[\bar{B} \rightarrow X_s \gamma, (E_\gamma > m_b/20)] &\simeq 3.70 \times 10^{-4}. \end{aligned} \quad (2)$$

In Fig. 1 the latter is compared to the measurements. In the near future the experimental error will reduce to approximately 5% which reduces the current error by almost a factor of two. Thus also the reduction of the theoretical uncertainty in Eq. (2) is mandatory.

<sup>\*</sup>To appear in the Proceedings of the International Conference and Loops and Legs in Quantum Field Theory 2004, Germany, 25-30 April 2004.

<sup>2</sup>The CLEO measurement from 1995 is not included in the average.

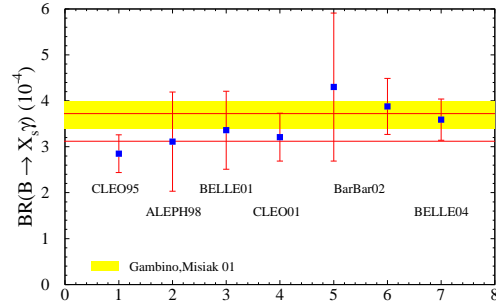


Figure 1. Comparison of the experimental measurements for BR( $\bar{B} \rightarrow X_s \gamma$ ), where a cut-off on the photon energy  $E_\gamma > m_b/20$  is applied, with the theoretical predictions given by the (yellow) band. The full (horizontal) lines indicate the uncertainties of the combined experimental results (cf. Eq. (1)).

At next-to-leading order (NLO) a detailed analysis of the theoretical error has been performed in Ref. [6]. It has been shown that the largest uncertainty comes from the dependence on the charm quark mass which arises for the first time at this order. Including all next-to-next-to-leading order (NNLO) effects one arrives at an uncertainty of approximately 7% which has to be compared with the 8% error quoted in Eq. (2). Thus a complete NNLO calculation can significantly reduce the theoretical uncertainty.

Calculations for the process  $\bar{B} \rightarrow X_s \gamma$  are conveniently performed within the framework of an effective theory where the scales of order  $M_W$  and higher are integrated out. This leads to an effective Lagrangian of the form

$$\mathcal{L}_{\text{eff}} = \mathcal{L}_{\text{QCD} \times \text{QED}}(u, d, s, c, b) \quad (3)$$

$$+ \frac{4G_F}{\sqrt{2}} \sum_{i,j} [V_{cs}^* V_{cb} C_i^c + V_{ts}^* V_{tb} C_i^t] Z_{ij} P_j,$$

where  $G_F$  is the Fermi constant,  $V$  stands for the Cabibbo-Kobayashi-Maskawa (CKM) matrix,  $P_j$  are the operators,  $C_i^{c/t}$  are the Wilson coefficients and  $Z_{ij}$  the corresponding renormalization constants. More details and explicit expressions can be found in [8] and references cited therein.

In such an effective-theory framework the calculation splits into three steps: (i) the matching of the full and the effective theory at the high scale, (ii) the evaluation of the operator matrix elements at the low scale  $m_b$ , and (iii) the running from the high to the low scale. At NNLO step (i) requires the evaluation of two-loop diagrams in order to obtain the matching coefficients for the four-fermion operators which has been performed in Ref. [9]. The three-loop matching coefficients  $C_7$  and  $C_8$  of the dimension-five dipole operators have been evaluated in Ref. [8] which will be considered in more detail in Section 2.

As far as the evaluation of the NNLO operator matrix elements are concerned up to now only the fermionic corrections of  $\mathcal{O}(\alpha_s^2 n_f)$  to  $P_1$ ,  $P_2$ ,  $P_7$  and  $P_8$  are known [10]. At NLO these operators are numerically important which is a strong motivation to consider the numerical effects at NNLO. Furthermore, once the corrections proportional to  $n_f$  are available, it is tempting to apply the so-called naive non-abelianization in order to estimate the complete corrections of order  $\alpha_s^2$ . This is based on the observation that the lowest coefficient of the QCD  $\beta$  function,  $\beta_0 = 11 - 2n_f/3$ , is quite large and thus it is expected that the replacement of  $n_f$  by  $-3\beta_0/2$  may lead to a good approximation of the full order  $\alpha_s^2$  corrections. In Section 3 we provide more details on this calculation. Finally, Section 4 contains our conclusions.

## 2. Three-loop contribution to $C_7$ and $C_8$

There are several possibilities to evaluate the matching coefficients. For instance, it is possible to evaluate the Feynman diagrams on-shell. However, we find it more convenient to follow the procedure outlined in Ref. [9] where all the necessary diagrams are evaluated off-shell, after expanding them in the external momenta. In intermediate steps spu-

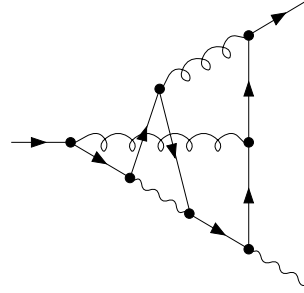


Figure 2. One of the  $\mathcal{O}(10^3)$  three-loop diagrams that contributes to  $b \rightarrow s\gamma$ .

rious infrared divergences appear which are generated by the expansion and are regulated dimensionally. They cancel out in the matching equation, i.e. in the difference between the full SM and the effective theory off-shell amplitudes.

The scalar three-loop integrals are evaluated with the help of the package MATAD [11] designed for calculating vacuum diagrams. The fact that MATAD can deal with a single non-vanishing mass only is not an obstacle against taking into account the actually different masses of the  $W$  boson and the top quark. Expansions starting from  $m_t = M_W$  and  $m_t \gg M_W$  allow us to accurately determine the three-loop matching conditions for the physical values of  $m_t$  and  $M_W$ .

The matching coefficients are obtained from the requirement that the one-particle-irreducible Green functions in the full and effective theory are equal. In the latter case only tree-level diagrams contribute as after expansion in the external momenta only scaleless integrals appear which are set to zero in dimensional regularization [12]. However, the counterterm contributions that arise from the effective-theory side have to be taken into account. On the SM side we have to consider of the order of 1000 three-loop diagrams. One of which is shown in Fig. 2. Obviously, when the virtual top quark is present in the open fermion line, we have to deal with three-loop vacuum integrals involving two mass scales,  $m_t$  and  $M_W$ . Also in the charm-quark sector such two-scale integrals are encountered when closed top-quark loops arise on the virtual gluon lines. At present, complete three-loop algorithms exist for vacuum integrals involving only a single mass scale. We have reduced

our calculation to such integrals by performing expansions around the point  $m_t = M_W$  and for  $m_t \gg M_W$ . In the latter case, the method of asymptotic expansions of Feynman integrals has been applied [13] which has been implemented in the C++ program `exp` [14]. At the physical point where  $M_W/m_t \approx 0.5$ , both expansions work reasonably well. This can be seen in Fig. 3 where the one-, two- and three-loop results for  $C_7$ , defined through

$$C_7^Q = C_7^{Q(0)} + \frac{\alpha_s}{4\pi} C_7^{Q(1)} + \dots, \quad (4)$$

( $Q = c, t$ ), are shown as functions of  $y = M_W/m_t(\mu_0)$ . (The plots for  $C_8$  show an analogous behaviour and can be found in Ref. [8].)

The variable  $y$  changes from 0 to 1, i.e. both starting points of our expansions are present in the figures. Note the relatively narrow ranges of the coefficient values on the vertical axes. The large  $m_t$  expansions (up to  $y^8$ ) are depicted by the dot-dashed lines, while the expansions around  $m_t = M_W$  (up to  $(1-y^2)^8$ ) are given by the dashed ones. In the one- and two-loop cases, solid curves show the exact results. The vertical strips mark the experimental values for  $y$ .

Comparing the three curves in the one- and two-loop cases, one can conclude that a combination of the two expansions at hand gives a good determination of the studied coefficients in the whole considered range of  $y$ .

Although we do not know the exact curves in the three-loop case, the same pattern seems to repeat. In fact, the charm-sector expansions perfectly overlap in the physical region. In the top sector, one can (conservatively) conclude that

$$C_7^{t(3)}(\mu_0 = m_t) = 12.05 \pm 0.05, \quad (5)$$

$$C_8^{t(3)}(\mu_0 = m_t) = -1.2 \pm 0.1, \quad (6)$$

which is perfectly accurate for any phenomenological application. Let us note that a change of  $C_7^{t(3)}(\mu_0 = m_t)$  from 12 to 13 would affect the  $b \rightarrow s\gamma$  decay width by only 0.02%, while a similar variation of  $C_8^{t(3)}(\mu_0 = m_t)$  would cause even a smaller effect. More detailed results can be found in Ref. [8].

### 3. Fermionic corrections to $P_1$ , $P_2$ , $P_7$ and $P_8$

The fermionic NNLO corrections of  $\mathcal{O}(\alpha_s^2 n_f)$  to  $P_1$ ,  $P_2$ ,  $P_7$  and  $P_8$  (cf. Ref. [

8] for their definition) require the evaluation of two- and three-loop diagrams where a light fermion loop is inserted into the gluon line. Sample diagrams are shown in Fig. 4.

The computation of the virtual corrections proceeds along the same lines as at NLO [15]. The essential difference is a modified gluon propagator which gets an additional  $\epsilon$ -dependent contribution  $1/p^{2\epsilon}$  arising from the light fermion loop.

The amplitudes of the contributing diagrams are constructed from one-loop building blocks describing the light-fermion insertion in the gluon propagator and the charm quark mass-dependent  $b\bar{s}g\gamma$ -vertex. Afterwards Feynman parameters are introduced. In the case of  $P_7$  and  $P_8$  the corresponding integrations can be performed analytically which is not possible for  $P_1$  and  $P_2$ . For the latter it is convenient to switch for the propagator involving the charm and the bottom quark mass to the Mellin-Barnes representations. This leads to a natural expansion in  $m_c/m_b$  which in practice converges very fast; the term of  $\mathcal{O}((m_c^2/m_b^2)^3)$  already leads to a negligible contribution.

The practical calculation in the case of  $P_7$  is slightly more involved as only the combination of the virtual corrections with the gluon bremsstrahlung and the quark-pair emission process is infrared safe. We decided to regulate the infrared singularities in the individual pieces by introducing a finite strange quark mass,  $m_s$ , and a mass of the quark in the fermion bubble,  $m_f$ . This enables several checks on intermediate results. In particular we could show that the sum of the virtual and the gluon bremsstrahlung corrections are finite in four dimensions in the limit  $m_s \rightarrow 0$  and for fixed  $m_f$ . The remaining dependence on  $m_f$  is canceled after including also the contribution from the quark-pair emission. Analytical results for the individual pieces can be found in Ref. [10], even for the case where a cut-off in the photon energy is introduced in the final phase space integration, which is important for the comparison with the experiment.

The numerical effect of the  $\mathcal{O}(\alpha_s^2 n_f)$  corrections is shown in Fig. 5. The corrections are moderate and amount to  $-3.9\%$  for  $\mu = 3.0$  GeV and to  $+3.4\%$  for  $\mu = 9.6$  GeV. Fig. 5 illustrates that the  $\mu$  dependence of the  $\mathcal{O}(\alpha_s^2 n_f)$  improved prediction for the branch-

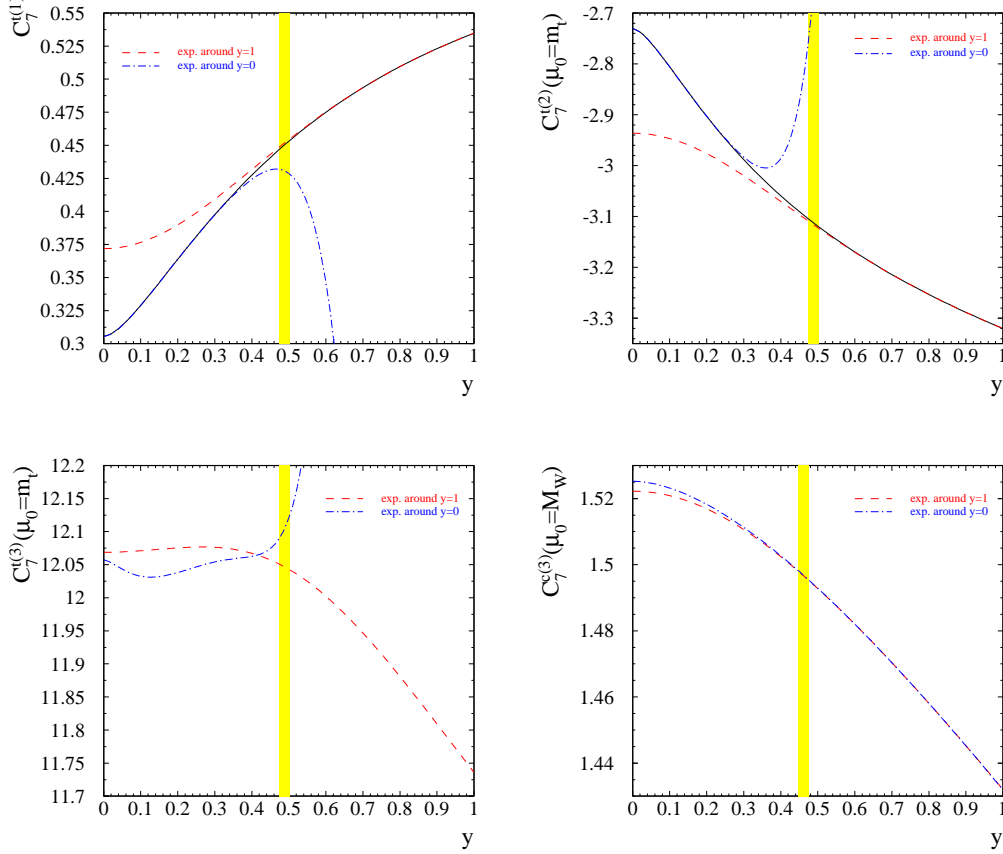


Figure 3. The coefficients  $C_7^{Q(n)}(\mu_0)$  as functions of  $y = M_W/m_t(\mu_0)$ . The (blue) dot-dashed lines correspond to their expansions in  $y$  up to  $y^8$ . The (red) dashed lines describe the expansions in  $(1-y^2)$  up to  $(1-y^2)^8$ . The (black) solid lines in the one- and two-loop cases correspond to the known exact expressions. The (yellow) vertical strips indicate the experimental range for  $y$ .

ing ratio is somewhat flatter than in the NLO case if we restrict ourselves to  $\mu \geq 4$  GeV. This is a welcome feature of our result, however, in general we cannot expect to reduce the  $\mu$  dependence as the solid curve only represents a part of the NNLO result. Indeed, we obtain a stronger  $\mu$ -dependence in the region below 4 GeV.

#### 4. Summary

In this contribution we reported on the first NNLO calculations to the branching ratio  $\text{BR}(\bar{B} \rightarrow X_s \gamma)$ . In particular, the three-loop matching calculations for  $C_7$  and  $C_8$  have been described [8]. Together with the two-loop calculation for the other relevant operators calculated several years ago [9] this com-

pletes the first step towards a complete NNLO analysis.

As far as the corrections to the operator matrix elements are concerned up to now only the fermionic corrections to the numerically most important operators  $P_i$  ( $i = 1, 2, 7, 8$ ) have been evaluated [10]. The remaining (virtual and real) corrections are not yet available. The same is true for the evaluation of the anomalous dimension to NNLO where diagrams up to four loops, from which the pole parts are needed, have to be computed.

It should be stressed that only the complete NNLO calculation, outlined after Eq. (3), leads to a scheme and scale independent result and is thus able to reduce the charm quark mass ambiguity.

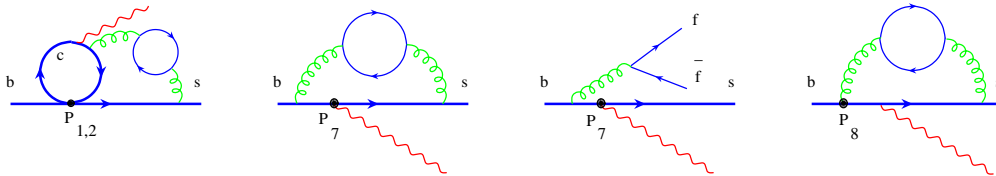


Figure 4. Sample diagrams contributing to the matrix elements of the operators  $P_i$  ( $i = 1, 2, 7, 8$ ). In the case of  $P_7$  next to the virtual corrections also the real radiation has to be considered.

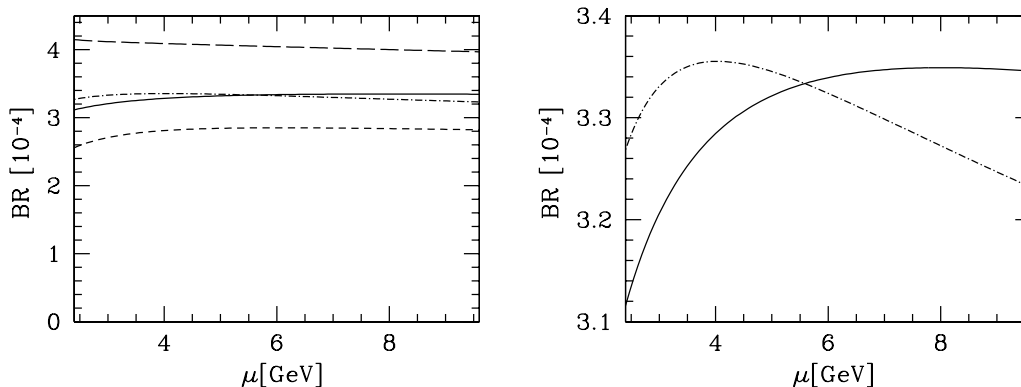


Figure 5. The branching ratio  $\text{BR}(\bar{B} \rightarrow X_s \gamma)$  as a function of the renormalization scale  $\mu$  where the plot on the right is an enlargement of the one on the left. The dash-dotted curve represents the NLO approximation and the solid curve includes the corrections of  $\mathcal{O}(\alpha_s^2 n_f)$ . For illustration in the left plot the latter are also shown for the case where the corrections to  $P_{1/2}$  ( $P_7$ ) are set to zero which corresponds to short-dashed (long-dashed) curve. A photon energy cut of  $E_{\text{cut}} = m_b/20$  is used, which corresponds to  $\delta = 0.9$ .

## Acknowledgements

I would like to thank K. Bieri, C. Greub and M. Misiak for fruitful collaborations on the subjects presented in this contribution. Furthermore, I would like to thank the organizers of Loops and Legs 2004 for the invitation and the nice conference. This work was supported by HGF Grant No. VH-NH-008.

## REFERENCES

1. S. Chen *et al.* (CLEO Collaboration), Phys. Rev. Lett. **87** (2001) 251807.
2. R. Barate *et al.* (ALEPH Collaboration), Phys. Lett. B **429** (1998) 169.
3. K. Abe *et al.* (BELLE Collaboration), Phys. Lett. B **511** (2001) 151.
4. B. Aubert *et al.* (BABAR Collaboration), [hep-ex/0207076].
5. C. Jessop, SLAC report SLAC-PUB-9610, November 2002; M. Misiak, private communication.
6. P. Gambino and M. Misiak, Nucl. Phys. B **611** (2001) 338.
7. A.J. Buras, A. Czarnecki, M. Misiak, and J. Urban, Nucl. Phys. B **631** (2002) 219.
8. M. Misiak and M. Steinhauser, Nucl. Phys. B **683** (2004) 277.
9. C. Bobeth, M. Misiak, and J. Urban, Nucl. Phys. B **574** (2000) 291.
10. K. Bieri, C. Greub, and M. Steinhauser, Phys. Rev. D **67** (2003) 114019.
11. M. Steinhauser, Comput. Phys. Commun. **134** (2001) 335.
12. In this context see: S. G. Gorishnii and S. A. Larin, Nucl. Phys. B **283** (1987) 452.
13. V. A. Smirnov, *Applied Asymptotic Expansions in Momenta and Masses*, Springer-Verlag, Heidelberg, 2001.
14. T. Seidensticker, hep-ph/9905298; R. Harlander, T. Seidensticker, and M. Steinhauser, Phys. Lett. B **426** (1998) 125.
15. C. Greub, T. Hurth, and D. Wyler, Phys. Rev. D **54** (1996) 3350.